Proceedings of the 26th IEEE Workshop on Control and Modeling of Power Electronics (COMPEL 2025),
June 22-26, 2025, Knoxville, TN, USA

Novel High-Power Isolated-Three-Phase-HF-Link Matrix-Type Three-Phase AC/DC Converter (i3X-Rectifier)

D. Zhang,
P. Sbabo,
D. Biadene,
P. Mattavelli,
J. W. Kolar

Novel Isolated-Three-Phase-HF-Link Matrix-Type Three-Phase AC/DC Converter (i3X-Rectifier)

Daifei Zhang†, Paolo Sbabo§, Davide Biadene§, Paolo Mattavelli§, and Johann W. Kolar*

† Department of Electrical & Computer Engineering, University of Toronto, Canada
§ Department of Management and Engineering, University of Padova, Italy
* Advanced Mechatronic Systems Group, ETH Zurich, Switzerland
E-Mail: daifei.zhang@utoronto.ca

***Abstract*—The rapid expansion of AI-driven data centers is significantly increasing the demand for ultra-efficient high-power three-phase (3-Φ) mains-connected single-stage ac/dc conversion solutions, featuring sinusoidal input current, galvanic isolation, and controlled output voltage. Conventional isolated-*single-phase*-HF-link matrix-type 3-Φ ac/dc converters encounter critical challenges at high power levels due to high component stresses. As a result, a relatively large number of low-power modules must be paralleled within a single 1 MW power rack, increasing system complexity and reducing reliability. To address this limitation, this paper introduces a novel isolated-*three-phase*-HF-link matriX-type three-phase ac/dc converter (i3X-Rectifier) that lowers individual component stresses and/or enhances power conversion efficiency and volumetric density in high-power, i.e., 100 kW range, data center power supplies. Utilizing a three-phase galvanic isolation transformer combined with either a direct or indirect matrix-type front-end, the proposed i3X-Rectifier enables single-stage (direct) conversion from 3-Φ low-frequency (LF) mains voltages to 3-Φ high-frequency (HF) transformer voltages, advantageously resulting in significantly reduced current stresses in main active and passive components and minimized filtering efforts. Furthermore, the proposed i3X-Rectifier supports quasi-current-dc-link operation, enabling generation of sinusoidal 3-Φ mains currents using conventional low-switching-loss current dc-link 2/3-PWM, simplifying modulation and reducing control complexity. Comprehensive closed-loop circuit simulations and comparative analyses of the proposed concept against the conventional isolated-*single-phase*-HF-link approach validate the substantial performance advantages of the proposed i3X-Rectifier, highlighting its suitability for next-generation high-power, high-efficiency data center power supply architectures.**

***Index Terms*—AI-Centric Data Center Power Supply, Electric Vehicle (EV) Charger, High-Power Single-Stage Isolated AC/DC Converter, Three-Phase Rectifier, Matrix-Type Converter, Dual Active Bridge (DAB), Isolated-Single-Phase-HF-Link, Isolated-Three-Phase-HF-Link**

I. Introduction

The rapid advancement of AI is driving an unprecedented surge in data center energy consumption. Modern AI training clusters, equipped with high-core-count CPUs and power-intensive GPU accelerators, consume up to 10 times more power than conventional server workloads [1]–[4]. This sharp increase in power demand necessitates a shift toward ±400 Vdc power distribution architecture to improve power efficiency and reduce the use of copper or aluminum, and/or to ensure better compatibility with emerging high-power AI infrastructure [5]–[7].

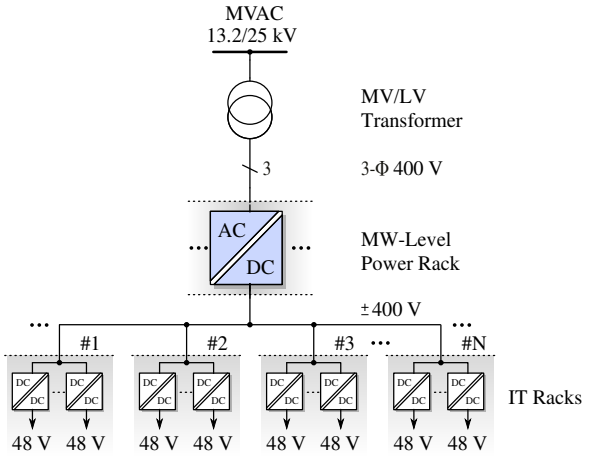

Fig. 1: Next-generation power distribution architecture for AI-centric data centers, highlighting the power delivery path from 13.2/25 kV medium-voltage ac (MVAC) to ±400 Vdc IT racks through dedicated advanced power racks. A single megawatt (MW)-level power rack needs to supply multiple IT payload racks employing multiple parallel-connected single-stage converter modules (see **Fig. 2**) providing sinusoidal input current rectification, galvanic isolation, and output voltage control functionalities.

Dedicated megawatt (MW)-level power racks will be employed to achieve ac/dc power conversion and provide galvanic isolation, enabling the delivery of ±400 Vdc to multiple IT payload racks, as shown in **Fig. 1**. Each MW-level power rack consists of parallel-connected isolated three-phase (3-Φ) ac/dc power converters. In this context, quasi-single-stage and single-stage isolated converter concepts are gaining traction due to their potentially lower power conversion losses and increased volumetric power densities [8]–[26].

However, typical isolated 3-Φ matrix-type ac/dc converters rely on isolated-*single-phase*-high-frequency(HF)-links (see **Fig. 2a**), i.e., are utilizing single-phase isolation transformers. This configuration presents significant limitations on high-power applications, primarily due to high transformer current stresses and substantial conduction losses of the individual power semiconductors. If, e.g., conventional single-stage isolated 3-Φ ac/dc power converters with 25 kW output are used as building blocks, more than 40 power modules must be coordinated to achieve a 1 MW output per power rack, without

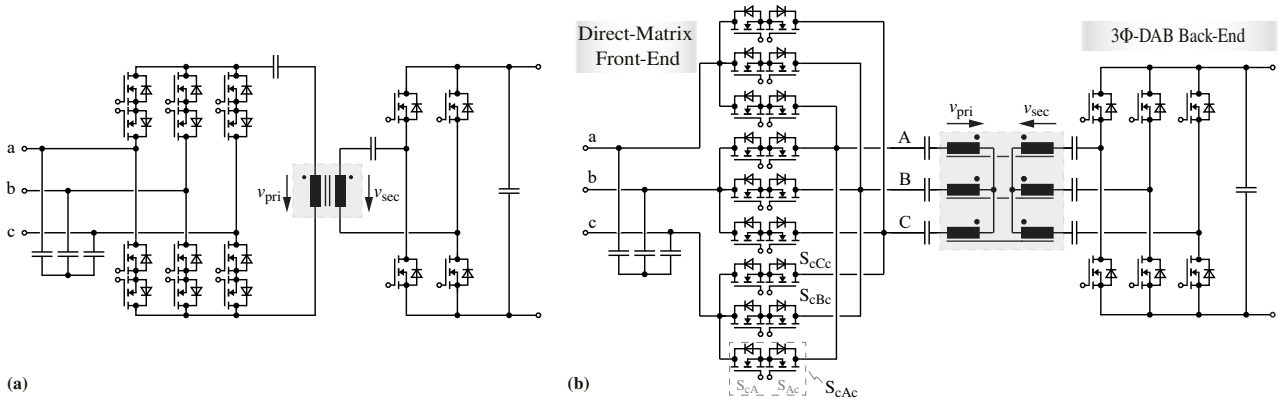

Fig. 2: Schematics of **(a)** a typical direct-matrix-type isolated-*single-phase*-HF-link 3-Φ ac/dc converter and **(b)** the proposed new direct-matrix-type isolated-*three-phase*-HF-link 3-Φ ac/dc converter, referred to as the **D-i3X-Rectifier**. The isolated-*three-phase*-HF-link, i.e., a three-phase transformer enables reduced component stresses (on power transistors and filter capacitors), lowers filtering requirements, and provides an extended soft-switching region [27], [28].

accounting for backup modules. This leads to significantly increased hardware complexity, potentially resulting in higher system costs and reduced operational reliability. Therefore, high-power (in the $100\,\mathrm{kW}$ range) output capability is essential for next-generation isolated 3-Φ ac/dc converters to ensure high efficiency and improved power density together with enhanced reliability.

To address these challenges, an isolated-*three-phase*-HF-link, rather than isolated-*single-phase*-HF-link, can be employed to enhance power-handling capability. This has been extensively studied in isolated dc/dc converter applications. Dual-active-bridge-type dc/dc converters with isolated-three-phase-HF-links, i.e., 3Φ-DAB-type dc/dc converters, can operate with significantly lower rms and peak current stresses, reduced magnetic flux harmonics, and minimized input/output filtering requirements, compared with 1Φ-DAB-type dc/dc converters delivering the same output power [27]–[29].

Therefore, this paper proposes a novel Direct isolated-three-phase-HF-link matriX-type 3-Φ ac/dc converter, referred to as D-i3X-Rectifier (see **Fig. 2b**). The D-i3X-Rectifier, derived in principle from 3Φ-DAB-type dc/dc converters, incorporates a three-phase isolation transformer to enhance performance and power efficiency in high-power applications.

The D-i3X-Rectifier interfaces the 3-Φ mains with a direct matrix-type front-end [30]–[32], allowing for direct LF-ac/HF-ac conversion from the 3-Φ mains voltages v_a, v_b, v_c to the three transformer primary-side voltages v_pri. Output voltage and power regulation are achieved by adjusting the phase shift applied to the 3Φ-DAB back-end, i.e., by fundamental DAB-type operation. This minimizes winding and core stresses while potentially enabling soft-switching (and allowing bidirectional power transfer). Consequently, the D-i3X-Rectifier emerges as a highly competitive solution for next-generation high-power data center and EV charger applications, particularly considering a realization utilizing $1200\,\mathrm{V}$ monolithic bidirectional bipolar switches [33]–[36], which are shown in **Fig. 2** as two inverse-series connected unipolar power MOSFETs.

Although multi-phase isolation transformers have been applied in matrix-type 3-Φ ac/dc converters [38]–[40], additional magnetic components, such as an output-side filter inductor or mains-side boost inductors have been employed alongside the isolation transformer, increasing converter costs and realization effort. Advantageously, the proposed D-i3X-Rectifier requires only a single magnetic component, i.e., a three-phase isolation transformer considering the DAB-type operation based on the transformer stray inductance, while achieving a true current-source behavior at the input and output interfaces, i.e., employing input and output capacitors directly connected to the switching stages.

The rest of this paper is organized as follows. **Section II** discusses the basic operating principle of the proposed D-i3X-Rectifier by leveraging the relations of the modulation schemes of the direct-matrix (ac/ac) front-end and a functionally equivalent indirect-matrix, i.e., ac/dc/ac input stage (see **Fig. 3a**). Simulation results ($10\,\mathrm{kW}$ output power, 3-Φ $400\,\mathrm{Vac}$ rms line-to-line input, and $400\,\mathrm{Vdc}$ output) are provided in **Section III** to validate the theoretical considerations, demonstrating sinusoidal 3-Φ mains currents and the generation of an isolated constant dc output voltage. **Section IV** provides a comparative stress analysis between a conventional matrix-type isolated-*single-phase*-HF-link 3-Φ ac/dc converter (see **Fig. 2a**) and the proposed i3X-Rectifier with an isolated-*three-phase*-HF-link (see **Fig. 2b**). Finally, **Section V** concludes the paper.

II. Operating Principle

This section first introduces the equivalence between the switching schemes of the direct-matrix front-end and an indirect-matrix converter input stage (the corresponding converter topology is referred to as I-i3X-Rectifier). Identical HF switching voltages can be generated at the terminals of the primary-side transformer with both topologies [30], [31]. Accordingly, identical voltage waveforms are generated across the three-phase isolation transformer, assuming identical control of the 3Φ-DAB back-end, which ultimately leads to the same mains-side input currents and dc output current.

To explain the operating principle of the I-i3X-Rectifier, a mains voltage relation of $v_\mathrm{a} > 0 > v_\mathrm{b} > v_\mathrm{c}$ is assumed, i.e., a 30° interval of the mains period is considered. The analysis for

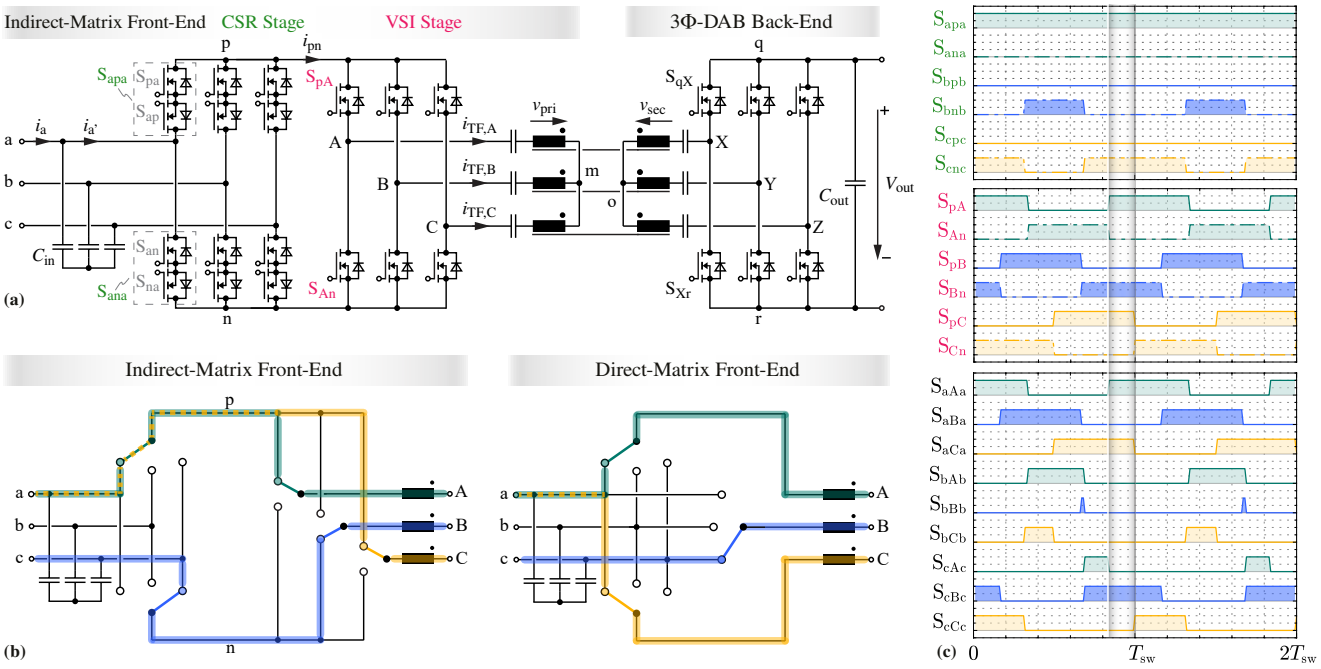

Fig. 3: **(a)** Indirect-matrix-type isolated-*three-phase*-HF-link 3-Φ ac/dc converter (**I-i3X-Rectifier**), consisting of an indirect-matrix front-end, i.e., a current source rectifier (CSR) stage and a voltage source inverter (VSI) stage. **(b)** Equivalence between the switching schemes of the direct-matrix and the indirect-matrix front-ends: the D-i3X-Rectifier front-end switching signals can be derived from the I-i3X-Rectifier front-end switching signals using (1), resulting in identical characteristic waveforms. **(c)** Switching signals of the D-i3X-Rectifier and the I-i3X-Rectifier over two switching periods. In the I-i3X-Rectifier, the CSR stage employs current dc-link 2/3-PWM [37] featuring low switching losses to generate an intermediate quasi-dc-link voltage v_{pn}, which is then converted into an HF-switched voltage v_{pri} by the VSI-stage to feed the isolated-*three-phase*-HF-link. The transformer's secondary side connects to a 3Φ-DAB back-end that delivers a constant dc output voltage.

the remaining intervals of the full mains cycle can be derived by cyclically interchanging the phase quantities.

A. Direct-Matrix & Indirect-Matrix Front-End

The relation and equivalence of the switching schemes of the direct-matrix and the indirect-matrix front-ends has been discussed in [30], [31] for 3-Φ motor drive applications. Each switching state of the direct-matrix front-end corresponds to a dedicated state of the indirect-matrix front-end.

For example, the direct-matrix front-end switching state with S_{aAa}, S_{cBc}, S_{aCa} in the turn-on state (see **Fig. 3b** and **Fig. 3c**) is equivalent to first turning on S_{apa} to connect the positive rail p to the input phase a and turning on S_{cnc} to connect the negative rail n to the input phase c, such that a quasi-dc-link voltage $v_{\text{pn}} = v_{\text{ac}}$ is impressed, considering the indirect-matrix front-end. Subsequently, v_{pn} is inverted by the voltage source inverter (VSI) stage such that the intermediate rail potentials p and n (and ultimately the input phase voltages) are connected to the corresponding primary winding terminals. E.g., turning on S_{pA} connects the positive rail p (the mains phase a) to the transformer terminal A, which is finally equivalent to gating S_{aAa} on. The same derivation can be applied to the winding terminals B and C.

The aforementioned equivalence between the switching states of the direct-matrix and indirect-matrix front-ends can be summarized as follows [30], [31]:

$$S_{\text{jKj}} = S_{\text{jpj}} \cdot S_{\text{pK}} + S_{\text{jnj}} \cdot S_{\text{Kn}}, \tag{1}$$

where $S \in \{1, 0\}$ indicates the on-state or off-state; j denotes one of the input phases a, b, c; K represents one of the transformer primary winding terminals A, B, C. This relation allows for a unique mapping of gate signals from the indirect-matrix front-end to the direct-matrix front-end. However, the reverse mapping (from the direct-matrix to the indirect-matrix front-end) has certain redundancies [30]–[32].

B. Modulation of the CSR Stage

The CSR stage of the I-i3X-Rectifier (see **Fig. 3a**) consists of two commutation cells, each comprising three bidirectional bipolar switches [41]. The switching state of the CSR stage is defined by the gated-on switches in the high-side and low-side commutation cells. For example, [ac] indicates that S_{apa} and S_{cnc} are turned on.

The CSR stage operates with current dc-link 2/3-PWM [37]. This approach advantageously ensures that each switching period consists of only two active switching states, i.e., does not include a (third) zero and/or freewheeling state, thereby minimizing the number of switching instants. As a result, the switching losses can be significantly reduced by roughly 70% [37], [41], [42]. For example, in the considered 30° interval (see **Fig. 4b**), rail p is always connected to phase a by continuously turning on S_{apa}. The active states [ab] and [ac] are alternatively applied within one switching period by turning either S_{bnb} or S_{cnc} on, respectively. Consequently, the quasi-dc-link voltage v_{pn} attains v_{ab} or v_{ac} in the considered 30° interval, as shown in **Fig. 4**.

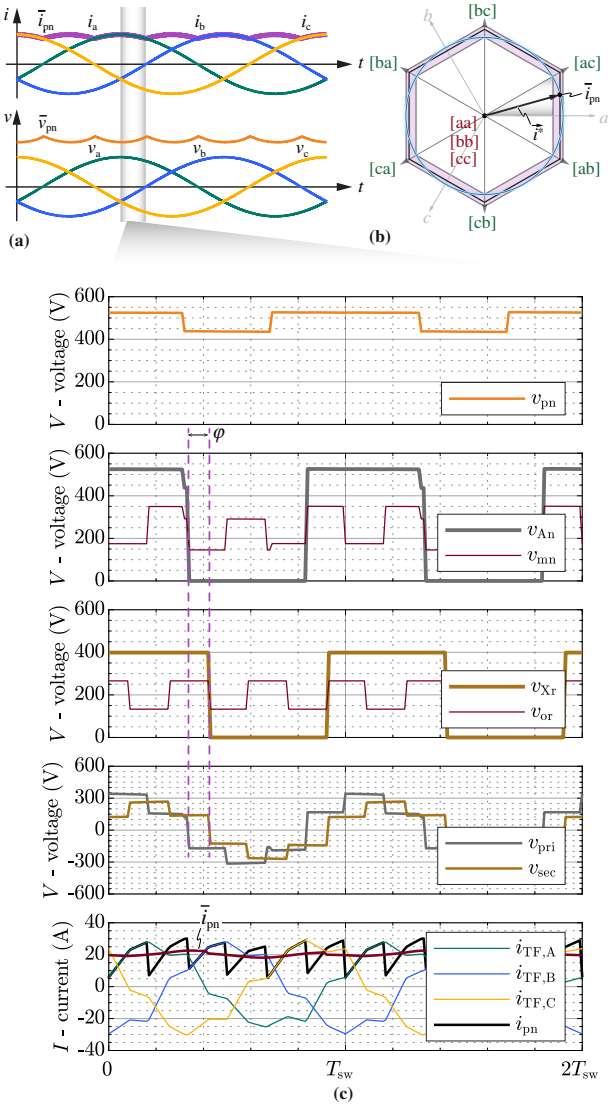

Fig. 4: **(a)** Considered 30° interval of a mains period with a mains voltage relation $v_a > 0 > v_b > v_c$ **(b)** Space-vector diagram of the current dc-link 2/3-PWM employed in the CSR stage, highlighting active (in green) and zero (in red) switching states, i.e., 2/3-PWM only uses active switching states [37]. **(c)** Characteristic waveforms of the I-i3X-Rectifier over two switching periods. The waveforms present the formation of primary v_{pri} and secondary v_{sec} winding voltages, whose difference drives the HF transformer currents $i_{TF,A}$, $i_{TF,B}$, $i_{TF,C}$, which follows a near-sinusoidal shape with very low HF harmonic content, enabling power transfer through the isolation transformer.

Furthermore, to ensure constant instantaneous power drawn from the 3-Φ mains, the local average value $\bar{i}_{pn}$ of the quasi-dc-link current follows the upper envelope of the 3-Φ mains current absolute values (see **Fig. 4a**). This required current is supplied by the downstream VSI stage.

C. Modulation of the VSI Stage & 3Φ-DAB Back-End

The bridge-legs of the VSI stage, operating with 120° interleaved and 50% duty cycle, convert the quasi-dc-link voltage v_{pn} into HF ac voltages applied to the transformer's primary terminals. Considering one of the phases, i.e., the transformer windings connected to the terminals A and X (see **Fig. 3a**), the primary-side winding voltage v_{pri} is given by

$$v_{pri} = v_{An} - v_{mn}, \tag{2}$$

where $v_{mn} = 1/3 \cdot (v_{An} + v_{Bn} + v_{Cn})$ represents the common-mode (CM) of the primary-side transformer terminal voltages and/or transformer star point n voltage (assuming a magnetically symmetric transformer construction). Note that the voltage across the series LF blocking capacitor C_s is neglected due to its relatively small magnitude.[1]

The 3Φ-DAB back-end is modulated in a similar manner as the VSI stage, i.e., using 120° interleaved 50% duty cycle modulation, which results in HF ac voltages across the transformer's secondary windings,

$$v_{sec} = v_{Xr} - v_{or}, \tag{3}$$

where $v_{or} = 1/3 \cdot (v_{Xr} + v_{Yr} + v_{Zr})$ is the CM component of the transformer's secondary-side terminal voltages.

Power transfer between the transformer's primary and secondary windings is regulated by the phase shift φ between the transformer voltages v_{pri} and v_{sec}. The voltage difference $v_{pri} - v_{sec}$ is applied across the transformer's stray inductance in each phase, finally driving transformer phase currents, e.g., $i_{TF,A}$, for power transfer through the isolated-three-phase-HF-link. Advantageously, $i_{TF,A}$ exhibits a waveform that is close to a sinusoidal shape, i.e., contains a low amount of HF current harmonics. This results in low HF ac losses in transformer windings and/or substantial improvements compared with the conventional matrix-type isolated-*single-phase*-HF-link 3-Φ ac/dc converter, where transformer currents are typically trapezoidal in shape, leading to higher harmonic content and increased (especially ac) winding losses, as discussed in **Section IV**.

For constant instantaneous power drawn from the 3-Φ mains, the local average value $\bar{i}_{pn}$ of the quasi-dc-link current must follow the upper envelope of the absolute values of the 3-Φ mains currents, forming a six-pulse-shaped waveform. The current i_{pn} is obtained by superimposing the 120° interleaved transformer currents $i_{TF,A}$, $i_{TF,B}$, $i_{TF,C}$, while accounting for the switching states of the VSI stage, as shown in **Fig. 4c**.

The quasi-dc-link current i_{pn} includes an HF switched component at $6f_{sw}$, whereas the carrier frequency of the 2/3-PWM is only f_{sw}. In other words, the duration of a single active switching state of the 2/3-PWM can span several periods of i_{pn}, allowing the charge impressed to the corresponding mains phase to be (relatively) accurately calculated using the local average $\bar{i}_{pn}$. Accordingly, although the HF ripple of i_{pn} cannot be entirely neglected, its impact on the formation of the sinusoidal 3-Φ mains currents is minimal.

[1]Note that the quasi-dc-link voltage v_{pn} alternates between two line-to-line voltages within each switching period, i.e., is not a constant dc voltage. Although the bridge-leg (S_{pA} and S_{An}) operates at a 50% duty cycle, an LF voltage component with relatively small magnitude ($< 20\,\mathrm{V}$) is generated. This LF voltage must be blocked by the series capacitor C_s. Accordingly, C_s must provide sufficient impedance in the LF range (which defines an upper bound for C_s), while C_s must show low impedance around the switching frequency (which defines a lower limit for C_s) to minimize its HF voltage ripple.

TABLE I: Main operating parameters and component specifications for the closed-loop circuit simulations. Note that L_{in}, L_σ, and L_{m} are not shown **Fig. 2**.

	Description	**Value**
V_{in}	RMS mains phase voltage	230 V
V_{out}	DC output voltage	400 V
P_{out}	Output power	10 kW
f_{sw}	Switching frequency	150 kHz
$N_{\text{p}} : N_{\text{s}}$	Transformer turns ratio	1:1
L_σ	Leakage inductance	7.5 µH
L_{m}	Magnetizing inductance	1 mH
C_{s}	Series capacitance	3 µF
L_{in}	Mains filter inductance	10 µH
C_{in}	Mains filter capacitance	18 µF
C_{out}	Output capacitance	20 µF

Therefore, current dc-link 2/3-PWM is sufficient to draw 3-Φ sinusoidal mains currents with minor distortion, and i_{pn} can be modulated similarly to the conventional HF-free dc-link current as in 3-Φ 2/3-PWM-controlled current source rectifiers [37], [41]. As a result, the proposed scheme, operating with the quasi-dc-link current i_{pn}, eliminates the need for dedicated charge control or look-up tables, typically required in matrix-type converters [9], [43], thereby significantly reducing control/firmware complexity.

To further mitigate current distortion in the I-i3X-Rectifier under quasi-dc-link current operation, a higher switching and/or carrier frequency can be used in the VSI stage compared with the CSR stage. This approach leverages the modulation degree of freedom enabled by decoupling the CSR and the VSI stages in the indirect-matrix front-end, rather than using a single direct-matrix front-end. A higher switching frequency ratio between the HF current components in i_{pn} and the CSR stage's carrier frequency and/or a more constant dc-link current can further suppress potential LF distortions in the 3-Φ mains currents.

III. Simulation Results

In this section, the operation of the I-i3X-Rectifier is validated through closed-loop circuit simulations, delivering 10 kW to a 400 Vdc load from 3-Φ 400 V mains. The main circuit specifications and parameters are listed in **Tab. I**. **Fig. 5a** - **Fig. 5b** present the proposed operating principle of the I-i3X-Rectifier, in which the 3-Φ sinusoidal mains currents are generated in phase and proportional to the corresponding measured 3-Φ input phase voltages. This confirms purely ohmic behavior at the 3-Φ mains interface.

In a 3Φ-DAB-type dc/dc converter, the power transferred across its isolation transformer is given by [27]:

$$\begin{aligned} P &= \frac{n \cdot V_{\text{dc1}} \cdot V_{\text{dc2}}}{2\pi f_{\text{sw}} L_\sigma} \cdot \frac{2}{3}\varphi \cdot \frac{4\pi - 3\varphi}{4\pi} \\ &= \frac{n \cdot V_{\text{dc1}} \cdot V_{\text{dc2}}}{2\pi f_{\text{sw}} L_\sigma} \cdot k_{3\Phi\text{-DAB}} \cdot \varphi, \end{aligned} \tag{4}$$

where V_{dc1} and V_{dc2} are the input and output dc voltages, n denotes the transformer turns ratio, and $k_{3\Phi\text{-DAB}}$ is a linearized coefficient in case of $0 < \varphi < \pi/3$.

Based on (4), the power transfer formula of the proposed I-i3X-Rectifier using current dc-link 2/3-PWM can be derived. The switching states of the CSR stage, together with the 3-Φ sinusoidal mains voltages, define the quasi-dc-link voltage v_{pn}. Although v_{pn} alternates between two line-to-line voltages within each switching period, due to linearity and the superposition theorem[2], the power transfer formula of the proposed I-i3X-Rectifier can be expressed as:

$$P = \frac{n \cdot \bar{v}_{\text{pn}} \cdot V_{\text{out}}}{2\pi f_{\text{sw}} L_\sigma} \cdot k_{3\Phi\text{-DAB}} \cdot \varphi, \tag{5}$$

where $\bar{v}_{\text{pn}}$ is the local average value of v_{pn}, which follows an inverse six-pulse shape as shown in **Fig. 5c**. The voltage across the series LF blocking capacitor C_{s} is again neglected due to its relatively small magnitude. Therefore, in steady-state operation, the phase shift φ between the matrix-type front-end and the 3Φ-DAB back-end follows a six-pulse shape (see **Fig. 5d**) to maintain constant power transfer.

Fig. 5e shows the primary v_{pri} and secondary v_{sec} transformer winding voltages, whose difference drives the transformer currents $i_{\text{TF,A}}$, $i_{\text{TF,B}}$, $i_{\text{TF,C}}$. These currents are then translated by the VSI stage into an impressed dc-link current, defining the quasi-dc-link current i_{pn} as shown in **Fig. 5f**. Note that the local average value $\bar{i}_{\text{pn}}$ follows a six-pulse-shaped waveform, forming the upper envelope of the absolute values of the 3-Φ mains currents over a mains fundamental period. This satisfies the requirement imposed by 2/3-PWM for maintaining (approximately) constant instantaneous power and ensuring that sinusoidal 3-Φ mains currents are drawn, as stated in **Section II-B**.

Fig. 5g illustrates the generation of 3-Φ sinusoidal mains currents. Taking phase a as an example, a pre-filter phase current $i_{\text{a'}}$ is obtained by modulating the quasi-dc-link current i_{pn} using 2/3-PWM. The HF current harmonics of $i_{\text{a'}}$ are filtered out by C_{in}, resulting in a (largely) sinusoidally-shaped phase current i_{a} that is proportional to the corresponding phase voltage v_{a}, thus achieving ohmic mains behavior of the I-i3X-Rectifier.

On the left-hand side of **Fig. 5h**, a switching period of the 30° interval (characterized by $v_{\text{a}} > 0 > v_{\text{b}} > v_{\text{c}}$ and/or CSR stage active switching states [ac], [ab]) is depicted. In this case, S_{apa} remains turned-on throughout the switching period, and $i_{\text{a'}} = i_{\text{pn}}$. Differently, on the right-hand side of **Fig. 5h**, the selected switching period employs the two active switching states [ac] and [bc]. In this case, $i_{\text{a'}} = i_{\text{pn}}$ holds during [ac]; whereas during [bc], both S_{apa} and S_{ana} are turned off so that $i_{\text{a'}}$ temporarily remains at 0 A.

[2]Considering the 30° interval of the mains period with a mains voltage relation $v_{\text{a}} > 0 > v_{\text{b}} > v_{\text{c}}$ as shown in **Fig. 4**, the power transfer of the proposed I-i3X-Rectifier can be expressed as:

$$\begin{aligned} P &= \frac{n \cdot (d_{\text{ac}} \cdot v_{\text{ac}} + d_{\text{ab}} \cdot v_{\text{ab}}) \cdot V_{\text{out}}}{2\pi f_{\text{sw}} L_\sigma} \cdot k_{3\Phi\text{-DAB}} \cdot \varphi \\ &= \frac{n \cdot \bar{v}_{\text{pn}} \cdot V_{\text{out}}}{2\pi f_{\text{sw}} L_\sigma} \cdot k_{3\Phi\text{-DAB}} \cdot \varphi, \end{aligned}$$

where d_{ac} and d_{ab} are the duty cycles of two active switching states [ac] and [ab], respectively, and v_{ac} and v_{ab} are the corresponding line-to-line voltages.

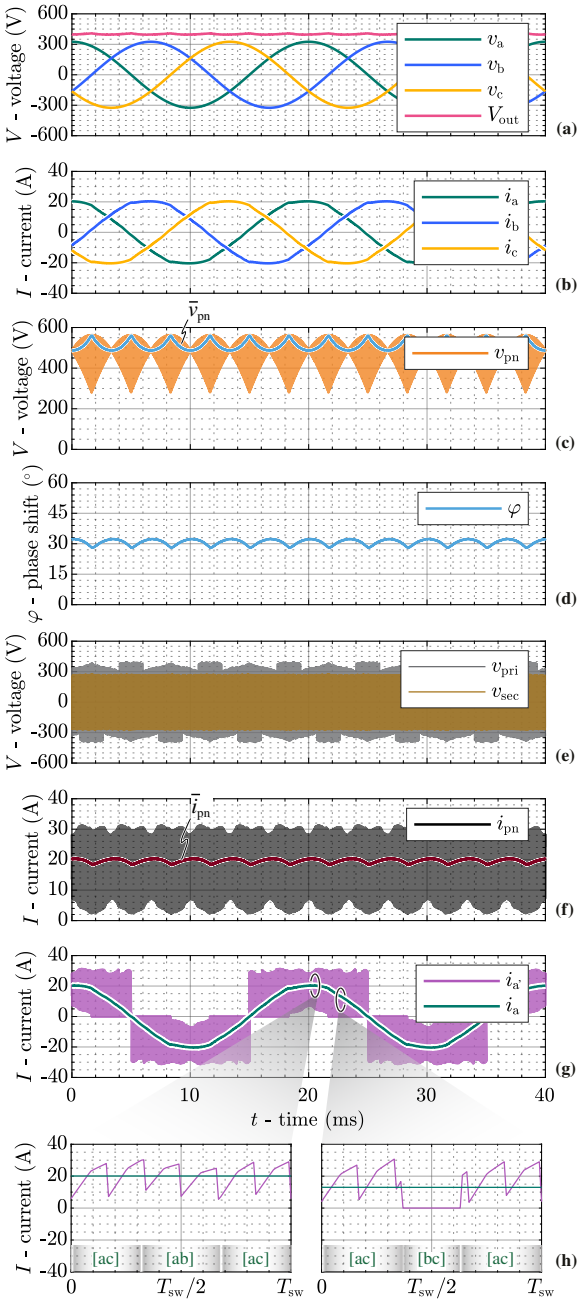

Fig. 5: Simulated key waveforms of the I-i3X-Rectifier connected to a 3-Φ 400 V mains, delivering a nominal power of 10 kW at 400 Vdc output. The output voltage (as well as the output power) is regulated by adjusting the phase shift φ applied to the carrier of the 3Φ-DAB back-end. Note that these presented key simulated waveforms of the I-i3X-Rectifier are identical to those of the proposed D-i3X-Rectifier for a given operating point and same system specifications.

IV. Component Stresses

This section provides a comparative analysis of the component stresses between the conventional matrix-type isolated-*single-phase*-HF-link 3-Φ ac/dc converter (see **Fig. 2a**) and the proposed i3X-Rectifier featuring an isolated-*three-phase*-HF-link (see **Fig. 3a**). Both converters operate at a switching frequency of 150 kHz and are connected to a 3-Φ 400 V mains, delivering a nominal power of 10 kW at 400 Vdc output.

TABLE II: RMS current stresses of the main components in the conventional matrix-type isolated-*single-phase*-HF-link 3-Φ ac/dc converter (see **Fig. 2a**) and the proposed i3X-Rectifiers with isolated-*three-phase*-HF-links. I_{matrix} and I_{DAB} denominate the rms current stresses of the primary-side and secondary-side power semiconductors.

	Stage / Component	Conv.	i3X-Rectifier
I_{matrix}	Front-end	16.1 A	12.1 A / 12.7 A || 10.4 A Indirect CSR / VSI || Direct
I_{DAB}	Back-end	19.6 A	12.6 A
I_{TF}	Isolation transformer	28.0 A	18.0 A
I_{Cin}	Input capacitor	14.1 A	9.0 A
I_{Cout}	Output capacitor	11.9 A	2.8 A

To ensure a fair comparison, both systems employ the same magnetizing inductance value L_{m}, while the leakage inductance of the i3X-Rectifier is adjusted to achieve a similar required phase shift φ for nominal power transfer. The analysis focuses on rms current stresses in key active and passive components, as well as magnetic core and winding stresses in the isolation transformers.

Both the I-i3X-Rectifier and the D-i3X-Rectifier are considered in this section. It is important to note that the stresses in the isolated-*three-phase*-HF-link and the 3Φ-DAB back-end are identical for both converters. The only distinction lies in the current stresses of matrix-type front-end stages.

A. Current Stresses

The rms current stresses are summarized in **Tab. II**, based on circuit simulation results. Both the proposed i3X-Rectifiers demonstrate largely reduced rms current stresses in active and passive components. Specifically, the switching-frequency interleaved operation of the phases leads to lower current stresses in the isolation transformer, as well as in the input and output capacitors, compared with those in the conventional matrix-type isolated-*single-phase*-HF-link 3-Φ ac/dc converter. This observation is consistent with previous findings in isolated dc/dc converter applications [27].

However, since both the proposed i3X-Rectifiers require a higher number of power semiconductors, the current stresses of the devices cannot be directly used for conduction loss comparisons. To enable a fair comparison, two scenarios are considered under different assumptions of semiconductor chip area. Note that the bipolar bidirectional switch (e.g., S_{cAc} in **Fig. 2** and S_{apa} in **Fig. 3**) used in the matrix-type front-ends are considered as a single device, with a shared drift region for blocking both voltage polarities, thereby requiring only a single chip area and/or the same chip area as, e.g., a unipolar switch of the VSI stage (of the I-i3X-rectifier). Additionally, for simplicity, the on-state resistance of each power switch is assumed to be inversely proportional to the chip area A_{chip}, regardless of the specific semiconductor material or packaging technology. The results are summarized in **Tab. III**.

In scenario **(a)**, an identical chip area A_{chip} **per switch** is assumed. The D-i3X-Rectifier generates approximately 60%

TABLE III: Ratio of conduction losses in the front-end and the back-end converter stage of the conventional matrix-type isolated-*single-phase*-HF-link 3-Φ ac/dc converter (see **Fig. 2a**) and the proposed i3X-Rectifiers, based on the current stresses listed in **Tab. II**. Two scenarios are considered: **(a)** same chip area per switch and **(b)** same total chip area per converter stage (see **Section IV-A** for further details).

Stage	**(a)** Same Area A_{chip} per Switch		**(b)** Same Total Area ΣA_{chip}	
Front-end	A_{chip} ratio	$P_{\text{cond.}}$ ratio	A_{chip} ratio	$P_{\text{cond.}}$ ratio
	1 : 1 : 1	1 : 1.19 : 0.63	$\frac{6}{6} : \frac{6}{12} : \frac{6}{9}$	1 : 2.37 : 0.94
Back-end	A_{chip} ratio	$P_{\text{cond.}}$ ratio	A_{chip} ratio	$P_{\text{cond.}}$ ratio
	1 : 1 : 1	1 : 0.62 : 0.62	$\frac{4}{4} : \frac{4}{6} : \frac{4}{6}$	1 : 0.93 : 0.93

Note: Provided sequence of **Conv. Matrix-Type : I-i3X-Rectifier : D-i3X-Rectifier**.

of the conduction losses observed in the conventional matrix-type isolated-*single-phase*-HF-link 3-Φ ac/dc converter. However, in the I-i3X-Rectifier, the transformer's primary winding currents must pass through two converter stages, i.e., the CSR and the VSI stages, before reaching the input 3-Φ mains. This results in approximately 20% higher conduction losses in the front-end stage, despite reduced rms currents in each individual device.

In scenario **(b)**, an identical **total** chip area ΣA_{chip} is allocated to either the front-end or the back-end stages, and is evenly distributed among all devices within the respective stage. Due to the increased number of components in both the front-end and back-end stages of both the proposed i3X-Rectifiers, the chip area A_{chip} per device is reduced, which results in higher on-state resistance for each switch.

For example, in the front-end stage, the conventional matrix-type isolated-*single-phase*-HF-link 3-Φ ac/dc converter consists of 6 switches with each assumed to have a unit chip area. In contrast, the indirect-matrix front-end (see **Fig. 3a**) employs a total of 12 switches, resulting in a chip area of $^6/_{12}$ per switch, i.e., effectively doubling the on-state resistance per device. The conduction losses ratio is then calculated based on the derived chip area per switch and the measured (simulated) currents in **Tab. II**.

Consequently, compared with scenario **(a)**, increased conduction losses are expected in the i3X-Rectifiers for scenario **(b)**. However, the D-i3X-Rectifier still advantageously achieves lower conduction losses in both converter stages compared with the conventional matrix-type isolated-*single-phase*-HF-link 3-Φ ac/dc converter.

B. Transformer Stresses

Comparisons between isolated-*single-phase*-HF-links and isolated-*three-phase*-HF-links have been conducted in the context of DAB-type dc/dc converters [27], [28], with results indicating that isolated-*three-phase*-HF-links offer improved overall performance. This section extends the analysis to isolated 3-Φ ac/dc converters and compares the isolated-*single-phase*-HF-link of the conventional matrix-type 3-Φ ac/dc converter (see **Fig. 6a**) and the isolated-*three-phase*-HF-link of the proposed i3X-Rectifiers (see **Fig. 6b**). Both systems are

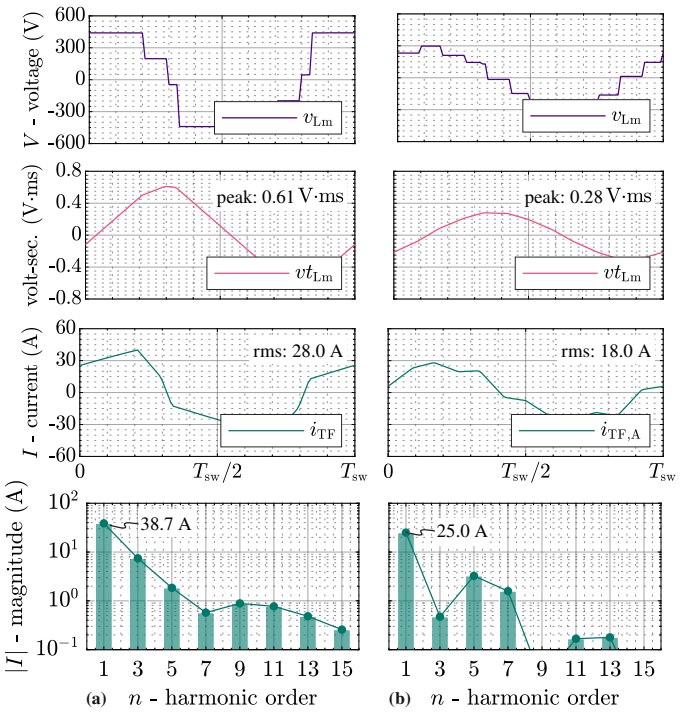

Fig. 6: Isolation transformer stresses including the magnetic flux waveforms, i.e., the voltage across the magnetizing inductance L_{m} (a T-type equivalent circuit and an equal splitting of the stray inductance L_σ between the primary and secondary side is assumed; for the i3X-Rectifiers a single phase of the three-phase transformer is considered) and its voltage-time integral (HF flux) vt_{Lm}, and winding current stresses, i.e., the transformer primary winding current i_{TF} and its spectrum, for **(a)** the isolated-*single-phase*-HF-link of the conventional matrix-type 3-Φ ac/dc converter and **(b)** the isolated-*three-phase*-HF-link of the proposed i3X-Rectifiers.

connected to a 3-Φ 400 V mains supply and deliver a nominal output power of 10 kW at 400 Vdc.

The voltage v_{Lm} across the magnetizing inductance L_{m} is first measured to evaluate the magnetic core stresses. In the proposed i3X-Rectifiers, v_{Lm} presents a more sinusoidal shape with extra voltage levels enabled by the three-phase and interleaved operation. Furthermore, a more sinusoidally-shaped transformer winding current i_{TF} is observed in the proposed i3X-Rectifiers, with significantly reduced peak and rms values. The reduced HF current harmonic content, as shown in the frequency spectra, leads to lower harmonic winding losses.

V. Conclusion

This paper introduces a novel isolated-*three-phase*-HF-link matrix-type 3-Φ ac/dc converter (**i3X-Rectifier**) for high-efficiency, high-power-density power supplies in next-generation AI data centers. Conventional isolated-*single-phase*-HF-link matrix-type 3-Φ ac/dc converters face scalability challenges in high-power applications due to excessive individual component stresses. The i3X-Rectifier leverages an isolated-*three-phase*-HF-link (a three-phase isolation transformer) along with a direct or indirect matrix-type front-end and 3Φ-DAB back-end, effectively mitigating these inherent limitations. Notably, the proposed i3X-Rectifier supports

quasi-dc-link current operation, i.e., the sinusoidal 3-Φ mains currents can be generated using established current dc-link 2/3-PWM, significantly simplifying modulation and reducing control complexity. Comprehensive closed-loop circuit simulation results confirm the expected performance improvements, including reduced current stresses in active and passive components, and close to sinusoidal transformer magnetic flux waveform, as well as lower input/output filtering efforts. These advantages position the proposed i3X-Rectifier as a promising solution for future high-power (in the 100 kW range) data center supplies in dedicated power racks and for high-power EV chargers.

REFERENCES

[1] McKinsey, "AI power: Expanding data center capacity to meet growing demand," https://www.mckinsey.com/industries/technology-media-and-telecommunications/our-insights/ai-power-expanding-data-center-capacity-to-meet-growing-demand/, accessed: 15-Nov-2024.

[2] Y. Chen, K. Shi, M. Chen, and D. Xu, "Data center power supply systems: From grid edge to point-of-load," *IEEE J. Emerg. Sel. Topics Power Electron.*, vol. 11, no. 3, pp. 2441–2456, Jun 2023.

[3] X. Xu and Q. Li, "Symmetric series-capacitor buck in 48 V-to-12 V regulated conversion for high-performance server boards," in *Proc. IEEE Energy Convers. Congr. Expo. (ECCE USA)*, Phoenix, AZ, USA, Oct. 2024, pp. 2583–2588.

[4] H. Li, W. Zeng, Y. Elasser, and M. Chen, "Air-LEGO: A magnetic-free ultra-thin 12 V-to-1 V 120 A VRM with air-coupled inductors," in *Proc. IEEE Appl. Power Electron. Conf. Expo. (APEC)*, Atlanta, GA, USA, Mar. 2025, pp. 510–517.

[5] X. Li, K. G. Ravikumar, and C. Peabody, "±400 V DC rack for AI/ML applications," in *Proc. of the Open Compute Project (OCP) Global Summit*, San Jose, CA, USA, Nov 2024.

[6] G. Deboy, M. Kasper, M. Wattenberg, and R. Rizzolatti, "Challenges and solutions to power latest processor generations for hyperscale datacenters," in *Proc. Int. Exhib. & Conf. Power Electron., Intell. Motion, Renew. Energy, & Energy Manag. (PCIM Europe)*, Nuremberg, Germany, Jun 2024.

[7] J. Huber, P. Wallmeier, R. Pieper, F. Schafmeister, and J. W. Kolar, "Comparative evaluation of MVAC-LVDC SST and hybrid transformer concepts for future datacenters," in *Proc. IEEE Int. Power Electron. Conf. (ECCE Asia)*, Himeji, Japan, May 2022.

[8] D. Das, K. Basu, N. Weise, R. Baranwal, and N. Mohan, "A bidirectional soft-switched DAB-based single-stage three-phase AC–DC converter for V2G application," *IEEE Trans. Transp. Electrification*, vol. 5, no. 1, pp. 186–199, 2019.

[9] L. Schrittwieser, M. Leibl, and J. W. Kolar, "99% efficient isolated three-phase matrix-type DAB buck–boost PFC rectifier," *IEEE Trans. Power Electron.*, vol. 35, no. 1, pp. 138–157, Jan 2020.

[10] M. Vazzoler, T. Caldognetto, D. Biadene, A. Petucco, and P. Mattavelli, "Isolated active front-end with integrated bidirectional GaN switches for battery chargers," in *Proc. IEEE Appl. Power Electron. Conf. Expo. (APEC)*, Long Beach, CA, USA, Feb 2024.

[11] R. Hao, S. Belkhode, J. Benzaquen, and D. Divan, "Multimode control of HF link universal minimal converters—Part I: Principles of operation," in *Proc. IEEE Energy Convers. Congr. Expo. (ECCE USA)*, Nashville, TN, USA, Oct. 2023.

[12] ——, "Multimode control of HF link universal minimal converters—Part II: Multiphase AC systems," in *Proc. IEEE Energy Convers. Congr. Expo. (ECCE USA)*, Nashville, TN, USA, Oct. 2023.

[13] T. Mishima and S. Mitsui, "A single-stage high-frequency-link modular three-phase LLC AC–DC converter," *IEEE Trans. Power Electron.*, vol. 37, no. 3, pp. 3205–3218, Mar. 2022.

[14] L. Gu, S. Chang, Y. Li, and X. Yang, "A single-stage fault-tolerant nine-bridge isolated three-phase bidirectional AC/DC converter and its SVPWM algorithm," *IEEE Trans. Ind. Electron.*, vol. 71, no. 12, pp. 15 804–15 814, Dec. 2024.

[15] Y. Wu, X. Wang, Z. Li, and J. Zhang, "Overview of single-stage high-frequency isolated AC–DC converters and modulation strategies," *IEEE Trans. Power Electron.*, vol. 38, no. 2, pp. 1583–1597, Feb. 2023.

[16] O. Korkh, A. Blinov, D. Vinnikov, and A. Chub, "Review of isolated matrix inverters: Topologies, modulation methods and applications," *Energies*, vol. 13, no. 9, p. 2394, May 2020.

[17] P. Sbabo, D. Biadene, P. Mattavelli, D. Zhang, and J. W. Kolar, "Ultra-efficient three-phase integrated-active-filter isolated rectifier for AI data center applications," in *Proc. IEEE Energy Convers. Congr. Expo. (ECCE Asia)*, Bengaluru, India, May 2025.

[18] H. Jeong, J. Lee, T. Song, and S. Choi, "Three-phase single-stage bi-directional electrolytic capacitor-less AC-DC converter with minimum switch count," in *Proc. IEEE Energy Convers. Congr. Expo.-Asia (ECCE Asia)*, Singapore, May 2021, pp. 2011–2015.

[19] D. Zhang, P. Sbabo, D. Biadene, P. Mattavelli, and J. W. Kolar, "Novel single-stage integrated active filter isolated matrix-type three-phase AC/DC converter (IAF-iMR)," in *Proc. IEEE Energy Convers. Congr. Expo. (ECCE Asia)*, Bengaluru, India, May 2025.

[20] W. Chen, R. Zane, D. Seltzer, and L. Corradini, "Isolated bidirectional DC/AC and AC/DC three-phase power conversion using series resonant converter modules and a three-phase unfolder," in *Proc. IEEE Workshop Control Model. Power Electron. (COMPEL)*, Columbus, OH, USA, Jun. 2014, pp. 1–6.

[21] P. Emiliani, A. Blinov, G. D. Carne, G. Arena, and D. Vinnikov, "Predictive control for isolated matrix rectifier without current distortion at sector boundary," in *Proc. IEEE Int. Conf. Compat. Power Electron. Power Eng. (CPE-POWERENG)*, Tallinn, Estonia, Jun. 2023, pp. 1–6.

[22] J. Afsharian, D. Xu, B. Wu, B. Gong, and Z. Yang, "A new PWM and commutation scheme for one phase loss operation of three-phase isolated buck matrix-type rectifier," *IEEE Trans. Power Electron.*, vol. 33, no. 11, pp. 9854–9865, Nov. 2018.

[23] C. Zhang, R. Wang, Z. Shen, T. Sadilek, A. Anurag, and P. Barbosa, "A single-stage three-phase isolated AC–DC converter for medium voltage solid state transformer applications," in *Proc. IEEE Appl. Power Electron. Conf. Expo. (APEC)*, Orlando, FL, USA, Mar. 2023, pp. 1503–1509.

[24] D. Zhang, S. Weihe, J. Huber, and J. W. Kolar, "Single-stage isolated bidirectional extended-functionality X-Rectifier for EV chargers with three/single-phase AC input capability," in *Proc. IEEE Energy Convers. Congr. Expo. (ECCE USA)*, 2024, pp. 2906–2913.

[25] M. Zhang, H. Zou, S. Farzamkia, C. Chen, and A. Q. Huang, "Three phase high-frequency-link-Y-configuration AC-DC DAB converter with monolithic bidirectional GaN switch," in *Proc. IEEE Energy Convers. Congr. Expo. (ECCE USA)*, Phoenix, AZ, USA, Oct. 2024, pp. 1130–1136.

[26] M. Liao, T. Sen, Y. Wu, and M. Chen, "Analysis and design of a cyclo-active-bridge inverter for single-stage three-phase grid interface," in *Proc. IEEE Appl. Power Electron. Conf. Expo. (APEC)*, Atlanta, GA, USA, Mar. 2025, pp. 139–146.

[27] R. De Doncker, D. Divan, and M. Kheraluwala, "A three-phase soft-switched high-power-density DC/DC converter for high-power applications," vol. 27, no. 1, pp. 63–73, Jan 1991.

[28] F. Krismer, "Modeling and optimization of bidirectional dual active bridge DC–DC converter topologies," PhD Thesis, ETH Zurich, 2010.

[29] J.-S. Hong, J.-I. Ha, S. Cui, and J. Hu, "Topology and control of an enhanced dual-active bridge converter with inherent bipolar operation capability for LVDC distribution systems," *IEEE Trans. Power Electron.*, vol. 38, no. 10, pp. 12 774–12 789, 2023.

[30] J. W. Kolar, T. Friedli, F. Krismer, and S. D. Round, "The essence of three-phase AC/AC converter systems," in *Proc. 13th Int. Power Electron. Motion Control Conf. (EPE-PEMC)*, Poznan, Poland, Sep. 2008, pp. 27–42.

[31] L. Huber and D. Borojevic, "Space vector modulated three-phase to three-phase matrix converter with input power factor correction," *IEEE Trans. Ind. Appl.*, vol. 31, no. 6, pp. 1234–1246, Nov. 1995.

[32] P. W. Wheeler, J. Rodriguez, J. C. Clare, L. Empringham, and A. Weinstein, "Matrix converters: A technology review," *IEEE Trans. Ind. Electron.*, vol. 49, no. 2, pp. 276–288, Apr. 2002.

[33] D. Bisi, "GaN bidirectional switches: The revolution is here," *IEEE Power Electron. Mag.*, vol. 12, no. 1, pp. 29–36, Mar. 2025.

[34] Y. Zhang, D. Dong, Q. Li, R. Zhang, F. Udrea, and H. Wang, "Wide-bandgap semiconductors and power electronics as pathways to carbon neutrality," *Nat. Rev. Electr. Eng.*, vol. 1, pp. 1–18, Jan. 2025.

[35] P. Das, C. Koller, and K. K. Leong, "Comparative analysis of CoolGaN™ BDS and B2B UDS dynamic on-resistance and switching loss performance," in *Proc. Int. Exhib. & Conf. Power Electron., Intell. Motion, Renew. Energy, & Energy Manag. (PCIM Europe)*, Nuremberg, Germany, May 2025.

[36] M. Basler, R. Reiner, D. Grieshaber, F. Benkhelifa, S. Müller, and S. Mönch, "Highly-integrated 1200 V GaN-based monolithic bidirectional switch," in *Proc. Int. Exhib. & Conf. Power Electron., Intell. Motion, Renew. Energy, & Energy Manag. (PCIM Europe)*, Nuremberg, Germany, May 2025.

[37] D. Zhang, J. Huber, and J. W. Kolar, "A three-phase synergetically controlled buck–boost current DC-link EV charger," *IEEE Trans. Power Electron.*, vol. 38, no. 12, pp. 15 184–15 198, Dec 2023.

[38] Z. Li, K. Jin, L. Gu, and C. Wang, "A buck-type isolated AC/DC converter for battery application," in *Proc. IEEE Annu. Southern Power Electron. Conf. (SPEC)*, Auckland, New Zealand, Dec. 2016, pp. 1–6.

[39] L. Gu and K. Peng, "A single-stage fault-tolerant three-phase bidirectional AC/DC converter with symmetric high-frequency Y-Δ connected transformers," *IEEE Trans. Power Electron.*, vol. 35, no. 9, pp. 9226–9237, Sep. 2020.

[40] J. Lee, H. Jeong, T.-T. Le, and S. Choi, "Three-phase single-stage bidirectional CCM soft-switching AC–DC converter with minimum switch count," *IEEE Trans. Power Electron.*, vol. 38, no. 2, pp. 2052–2062, Feb. 2023.

[41] D. Zhang, M. Leibl, J. Muhlethaler, J. Huber, and J. W. Kolar, "Analytical modeling and comparison of EMI pre-filter noise emissions of three-phase voltage and current DC-link converters," *IEEE Trans. Power Electron.*, vol. 39, no. 4, pp. 4567–4581, Apr. 2024.

[42] S. Weihe, D. Menzi, J. Huber, D. Zhang, J. W. Kolar, M. Kasper, K. K. Leong, and G. Deboy, "Novel bidirectional single-stage isolated 600 V GaN M-BDS-based single-/three-phase-operable EV on-board charger," in *Proc. Int. Exhib. & Conf. Power Electron., Intell. Motion, Renew. Energy, & Energy Manag. (PCIM Europe)*, Nuremberg, Germany, Jun. 2024, pp. 330–337.

[43] K. M. Smedley and S. Ćuk, "One-cycle control of switching converters," *IEEE Trans. Power Electron.*, vol. 10, no. 6, pp. 625–633, Nov. 1995.